

Performance Measures in Electric Power Networks under Line Contingencies

Tommaso Coletta, and Philippe Jacquod, *Member, IEEE*

Abstract—Classes of performance measures expressed in terms of \mathcal{H}_2 -norms have been recently introduced to quantify the response of coupled dynamical systems to external perturbations. For the specific case of electric power networks, these measures quantify for instance the primary effort control to restore synchrony, the amount of additional power that is ohmically dissipated during the transient following the perturbation or, more conceptually, the coherence of the synchronous state. So far, investigations of these performance measures have been restricted to nodal perturbations. Here, we go beyond earlier works and consider the equally important, but so far neglected case of line perturbations. We consider a network-reduced power system, where a Kron reduction has eliminated passive buses. Identifying the effect that a line fault in the physical network has on the Kron-reduced network, we find that performance metrics depend on whether the faulted line connects two passive, two active buses or one active to one passive bus. In all cases, performance metrics depend quadratically on the original load on the faulted line times a topology dependent factor. Our theoretical formalism being restricted to Dirac- δ perturbations, we investigate numerically the validity of our results for finite-time line faults. We find good agreement with theoretical predictions for longer fault durations in systems with more inertia.

Index Terms—Power generation control, power system dynamics performance measures, line contingency.

I. INTRODUCTION

In normal operation, electric power grids are synchronized. Their operating state corresponds to equal frequencies and voltage angle differences ensuring power conservation at all buses. Such synchronous states are not specific to power grids. They occur in many different coupled dynamical systems, depending on the balance between the internal dynamics of the individual systems and the coupling between them [1], [2]. For the specific case of electric power grids, the individual systems are either generators or loads, and they are coupled to one another by power lines. Individual units have effective internal dynamics determined by their nature – they may be rotating machines, inertialess new renewable energy sources, load impedances and so forth – and by the amount of power they generate or consume [3]. Rapid changes are currently affecting the structure of power grids which will no doubt impact their operating states [4]. With higher penetration levels of renewable energy sources, generations become decentralized, they have less inertia and they fluctuate more strongly [5]. Future power grids will be subjected more often to stronger external perturbations to which they may react more strongly.

There is thus a clear need to better assess power grid vulnerability. Investigations have been initiated on the robustness of the synchronous operating state of electric power grids to external perturbations. An approach has been advocated in consensus and synchronization studies [6]–[9], which starts from a stable operating state, perturbs it and quantifies the magnitude of the induced transient excursion through various performance measures. Focusing on Dirac- δ , nodal perturbations – instantaneous changes in generation or consumption – quadratic performance measures have been proposed, which can be formulated as \mathcal{L}_2 and squared \mathcal{H}_2 norms of linear systems. The approach is mathematically elegant because these norms can be conveniently expressed in terms of observability Gramians [10]. Exported to electric power grids, performance measures allow to evaluate additional transmission losses incurred during the transient as synchronous machines oscillate relative to one another, [11], [12], or the primary control effort necessary to restore synchrony [13]. Under the assumptions that synchronous machines have uniform inertia and damping coefficients, and that transmission lines are homogeneous – that they have constant resistance over reactance ratios – Ref. [11] obtained that additional transmission losses depend only on the number of buses in the network, and not on its topology. Relaxing the homogeneous line assumption, Ref. [12] related the same performance measure to a graph theoretical distance metric known as the resistance distance [14], [15]. To the best of our knowledge, investigations of performance measures of synchronized states have considered nodal perturbations only. In this manuscript, we extend these investigations to line contingencies which are at least as important for evaluating the robustness of electric power grids.

The main contribution of our work is to extend the observability Gramian formalism to assess performance measures for transients caused by line contingencies. In this case, the perturbation acts on the network Laplacian matrix, it is thus a multiplicative perturbation, a priori fundamentally different and harder to treat than the additive nodal perturbations considered so far. A second difficulty we overcome is that analytical results can be obtained only for uniform inertia to damping ratio, forcing us to consider Kron-reduced networks without inertialess passive nodes. To consider relevant line contingencies, we therefore need to map single-line faults in the physical network onto the Kron-reduced network. Our results differentiate between faults on power lines connecting two passive nodes, two active nodes, or one passive to one active node in the physical network. Because we consider Dirac- δ perturbations, we compare our theory to numerical simulations with finite-time line faults. We confirm our ana-

T. Coletta and Ph. Jacquod are with the School of Engineering of the University of Applied Sciences of Western Switzerland CH-1951 Sion, Switzerland. Emails: (tommaso.coletta, philippe.jacquod)@hevs.ch.

lytical results for finite-time fault lasting typically up to few AC cycles. We find that the agreement between theoretical Dirac- δ and numerical perturbations is better for longer fault durations in systems with larger inertias.

The works mentioned above focus on performance measures that are relevant to AC electric power networks and which can be computed analytically as \mathcal{H}_2 norms for a state-space system. Generally, the observability Gramian required to evaluate \mathcal{H}_2 norms is defined implicitly by a Lyapunov equation which is typically solved numerically. A secondary contribution of our work is to derive an analytic solution of the Lyapunov equation valid for generic performance measures, under the assumption that synchronous machines have uniform damping over inertia ratios. By revisiting some of the results of Refs. [11], [12] and [13], we show how specific assumptions lead to performance measures that no longer depend on the network topology, and clarify the mathematical mechanism by which this occurs. Our results allow to compute other performance measures and to interpret them in terms of the average resistance distance [14], [15] a quantity also known as the inverse closeness centrality [16].

This paper is organized as follows. Section II introduces the mathematical notations and defines the effective resistance distance. The high voltage AC electric network model, and the observability Gramian formalism are outlined in Sec. III. Section IV derives a closed-form expression for the observability Gramian in general cases. The broad range of applicability of our results for the observability Gramian is illustrated by evaluating a variety of network performance measures in Sec. V. The new application of the Gramian formalism to line contingencies is discussed in Sec. VI and is supported by the numerical simulations presented in Sec. VII. A brief conclusion is given in Sec. VIII.

II. MATHEMATICAL NOTATION

Given the vector $\mathbf{v} \in \mathbb{R}^N$ and the matrix $\mathbf{M} \in \mathbb{R}^{N \times N}$ we denote their transpose by \mathbf{v}^\top and \mathbf{M}^\top . For any two vectors $\mathbf{u}, \mathbf{v} \in \mathbb{R}^N$, $\mathbf{u}\mathbf{v}^\top$ is the matrix in $\mathbb{R}^{N \times N}$ having as i, j th component the scalar $u_i v_j$ and $\text{diag}(\{v_i\})$ denotes the diagonal matrix having v_1, \dots, v_N as diagonal entries. Let $\hat{\mathbf{e}}_l \in \mathbb{R}^N$ with $l \in \{1, \dots, N\}$ denote the unit vector with components $(\hat{\mathbf{e}}_l)_i = \delta_{il}$. We define $\mathbf{e}_{(l,q)} \in \mathbb{R}^N$ as $\mathbf{e}_{(l,q)} = \hat{\mathbf{e}}_l - \hat{\mathbf{e}}_q$.

We denote undirected weighted graphs by $\mathcal{G} = (\mathcal{N}, \mathcal{E}, \mathcal{W})$ where \mathcal{N} is the set of its N vertices, \mathcal{E} is the set of edges, and $\mathcal{W} = \{w_{ij}\}$ is the set of edge weights, with $w_{ij} = 0$ whenever i and j are not connected by an edge, and $w_{ij} = w_{ji} > 0$ otherwise. The graph Laplacian $\mathbf{L} \in \mathbb{R}^{N \times N}$ is the symmetric matrix given by $\mathbf{L} = \sum_{i < j} w_{ij} \mathbf{e}_{(i,j)} \mathbf{e}_{(i,j)}^\top$. We denote by $\{\lambda_1, \dots, \lambda_N\}$ and $\{\mathbf{u}^{(1)}, \dots, \mathbf{u}^{(N)}\}$ the eigenvalues and orthonormalized eigenvectors of \mathbf{L} . The zero row and column sum property of \mathbf{L} implies that $\lambda_1 = 0$ and that $\mathbf{u}^{(1)} = (1, \dots, 1)/\sqrt{N}$. All remaining eigenvalues of \mathbf{L} are strictly positive in connected graphs $\lambda_i > 0$ for $i = 2, \dots, N$. The orthogonal matrix $\mathbf{T} \in \mathbb{R}^{N \times N}$ having $\mathbf{u}^{(i)}$ as i th column diagonalizes \mathbf{L} , i.e. $\mathbf{T}^\top \mathbf{L} \mathbf{T} = \mathbf{\Lambda}$ where $\mathbf{\Lambda} = \text{diag}(\{\lambda_i\})$. The Moore-Penrose pseudoinverse of \mathbf{L} is given by $\mathbf{L}^\dagger = \mathbf{T} \text{diag}(\{0, \lambda_2^{-1}, \dots, \lambda_N^{-1}\}) \mathbf{T}^\top$ and is such that

$\mathbf{L} \mathbf{L}^\dagger = \mathbf{L}^\dagger \mathbf{L} = \mathbb{I} - \mathbf{u}^{(1)} \mathbf{u}^{(1)\top}$ with $\mathbb{I} \in \mathbb{R}^{N \times N}$ denoting the identity matrix.

The effective resistance distance between any two nodes i and j of the network is defined as $\Omega_{ij} = \mathbf{e}_{(i,j)}^\top \mathbf{L}^\dagger \mathbf{e}_{(i,j)}$ [14], [15]. This quantity is a graph theoretical distance metric satisfying the properties: i) $\Omega_{ii} = 0 \forall i \in \mathcal{N}$, ii) $\Omega_{ij} \geq 0 \forall i \neq j \in \mathcal{N}$, and iii) $\Omega_{ij} \leq \Omega_{ik} + \Omega_{kj} \forall i, j, k \in \mathcal{N}$. It is known as the *resistance* distance because if one replaces the edges of \mathcal{G} by resistors with a conductance $1/R_{ij} = w_{ij}$, then Ω_{ij} is equal to the equivalent network resistance when a current is injected at node i and extracted at node j with no injection anywhere else. The expression of the resistance distance in terms of the eigenvalues and eigenvectors of \mathbf{L} is given by $\Omega_{ij} = \sum_{l \geq 2} \lambda_l^{-1} (u_i^{(l)} - u_j^{(l)})^2$ [17]–[19].

III. POWER NETWORK MODEL AND QUADRATIC PERFORMANCE MEASURES

We consider high voltage transmission power networks in the DC approximation (i.e. constant voltage magnitudes, purely susceptive transmission lines and small voltage phase differences). The steady state power flow equations relating the active power injections \mathbf{P} to the voltage phases $\boldsymbol{\theta}$ at every node read $\mathbf{P} = \mathbf{L}_b \boldsymbol{\theta}$. Here, \mathbf{L}_b is the Laplacian matrix of the graph modeling the electric network and whose edge weights are given by the susceptances of the transmission lines $w_{ij} = b_{ij} \geq 0$. We assume that each node of the network has a synchronous machine (generator or consumer) of rotational inertia $m_i > 0$ and damping coefficient $d_i > 0$. The network dynamics is governed by the *swing* equations [3]. In the frame rotating at the nominal frequency of the network they read

$$\mathbf{M} \ddot{\boldsymbol{\theta}} = -\mathbf{D} \dot{\boldsymbol{\theta}} + \mathbf{P} - \mathbf{L}_b \boldsymbol{\theta}, \quad (1)$$

with $\mathbf{M} = \text{diag}(\{m_i\})$ and $\mathbf{D} = \text{diag}(\{d_i\})$. Subject to a power injection perturbation $\delta \mathbf{p}(t)$, the system deviates from the nominal operating point $(\boldsymbol{\theta}^*, \boldsymbol{\omega}) := (\mathbf{L}_b^\dagger \mathbf{P}, 0)$ according to $\boldsymbol{\theta}(t) = \boldsymbol{\theta}^* + \delta \boldsymbol{\theta}(t)$, and $\boldsymbol{\omega}(t) = \delta \dot{\boldsymbol{\theta}}(t)$. The swing dynamics is determined by

$$\begin{bmatrix} \delta \dot{\boldsymbol{\theta}} \\ \dot{\boldsymbol{\omega}} \end{bmatrix} = \begin{bmatrix} 0 & \mathbb{I} \\ -\mathbf{M}^{-1} \mathbf{L}_b & -\mathbf{M}^{-1} \mathbf{D} \end{bmatrix} \begin{bmatrix} \delta \boldsymbol{\theta} \\ \boldsymbol{\omega} \end{bmatrix} + \begin{bmatrix} 0 \\ \mathbf{M}^{-1} \delta \mathbf{p} \end{bmatrix}. \quad (2)$$

Using $\bar{\delta \boldsymbol{\theta}} = \mathbf{M}^{1/2} \delta \boldsymbol{\theta}$ and $\bar{\boldsymbol{\omega}} = \mathbf{M}^{1/2} \boldsymbol{\omega}$ we rewrite Eq. (2) as

$$\begin{bmatrix} \dot{\bar{\delta \boldsymbol{\theta}}} \\ \dot{\bar{\boldsymbol{\omega}}} \end{bmatrix} = \underbrace{\begin{bmatrix} 0 & \mathbb{I} \\ -\mathbf{M}^{-1/2} \mathbf{L}_b \mathbf{M}^{-1/2} & -\mathbf{M}^{-1} \mathbf{D} \end{bmatrix}}_{\mathbf{A}} \begin{bmatrix} \bar{\delta \boldsymbol{\theta}} \\ \bar{\boldsymbol{\omega}} \end{bmatrix} + \begin{bmatrix} 0 \\ \mathbf{M}^{-1/2} \delta \mathbf{p} \end{bmatrix}, \quad (3)$$

which symmetrizes the four blocks of the stability matrix \mathbf{A} . Eqs. (2) and (3) capture the transient dynamics resulting from the perturbation $\delta \mathbf{p}(t)$. For asymptotically stable systems and perturbations that are short and weak enough that they leave the dynamics inside the basin of attraction of $\boldsymbol{\theta}^*$, the operating point will eventually return to $(\delta \boldsymbol{\theta}, \boldsymbol{\omega}) = (0, 0)$.

We want to characterize the transient by evaluating quadratic performance measures of the type

$$\mathcal{P} = \int_0^\infty [\delta \boldsymbol{\theta}^\top \boldsymbol{\omega}^\top] \mathbf{Q} \begin{bmatrix} \delta \boldsymbol{\theta} \\ \boldsymbol{\omega} \end{bmatrix} dt, \quad \mathbf{Q} = \begin{bmatrix} \mathbf{Q}^{(1,1)} & 0 \\ 0 & \mathbf{Q}^{(2,2)} \end{bmatrix} \quad (4)$$

where we assumed that $\delta \mathbf{p}(t)$ is such that $\delta \mathbf{p}(t < 0) = 0$ and the symmetric matrix $\mathbf{Q} \in \mathbb{R}^{2N \times 2N}$ depends on the specific performance measure to investigate. For Dirac- δ perturbations $\delta \mathbf{p}(t) = \delta(t) \mathbf{p}_0$ and initial conditions $(\delta \boldsymbol{\theta}(0), \boldsymbol{\omega}(0)) = (0, 0)$, Eq. (3) is explicitly solved yielding

$$\begin{bmatrix} \delta \boldsymbol{\theta}(t) \\ \bar{\boldsymbol{\omega}}(t) \end{bmatrix} = e^{\mathbf{A}t} \underbrace{\begin{bmatrix} 0 \\ \mathbf{M}^{-1/2} \mathbf{p}_0 \end{bmatrix}}_{\mathbf{B}}. \quad (5)$$

The performance measure \mathcal{P} , Eq. (4), can be expressed as

$$\mathcal{P} = \mathbf{B}^\top \mathbf{X} \mathbf{B}, \quad (6)$$

with the observability Gramian $\mathbf{X} = \int_0^\infty e^{\mathbf{A}^\top t} \mathbf{Q}^M e^{\mathbf{A}t} dt$, and

$$\mathbf{Q}^M = \begin{bmatrix} \mathbf{M}^{-1/2} \mathbf{Q}^{(1,1)} \mathbf{M}^{-1/2} & 0 \\ 0 & \mathbf{M}^{-1/2} \mathbf{Q}^{(2,2)} \mathbf{M}^{-1/2} \end{bmatrix}. \quad (7)$$

For asymptotically stable systems (i.e. when all eigenvalues of \mathbf{A} have negative real part), the observability Gramian \mathbf{X} satisfies the Lyapunov equation

$$\mathbf{A}^\top \mathbf{X} + \mathbf{X} \mathbf{A} = -\mathbf{Q}^M. \quad (8)$$

For Laplacian systems, $\sum_i (\mathbf{L}_b)_{ij} = \sum_j (\mathbf{L}_b)_{ij} = 0$, therefore \mathbf{A} has a marginally stable mode $\mathbf{A}[\mathbf{M}^{1/2} \mathbf{u}^{(1)}, 0]^\top = 0$. The standard approach to deal with this marginally stable mode is to consider performance measures \mathbf{Q} such that $\mathbf{u}^{(1)} \in \ker(\mathbf{Q}^{(1,1)})$, in which case the observability Gramian is well defined by Eq. (8) with the additional constraint $\mathbf{X}[\mathbf{M}^{1/2} \mathbf{u}^{(1)}, 0]^\top = 0$ [13]. In this work, we propose a new approach to treat the marginally stable mode by introducing a regularizing parameter in the Laplacian making it nonsingular.

Proposition 1. *The Laplacian \mathbf{L}_b under the transformation $\mathbf{L}_b \rightarrow \mathbf{L}_b + \epsilon \mathbb{I}$ with $\epsilon > 0$ is non singular and its inverse is*

$$\mathbf{L}_b^{-1} = \mathbf{T} \text{diag}(\{\epsilon^{-1}, (\lambda_2 + \epsilon)^{-1}, \dots, (\lambda_N + \epsilon)^{-1}\}) \mathbf{T}^\top, \quad (9)$$

where λ_i 's and \mathbf{T} are the eigenvalues and the orthogonal matrix diagonalizing \mathbf{L}_b for $\epsilon = 0$.

Proof. The effect of $\mathbf{L}_b \rightarrow \mathbf{L}_b + \epsilon \mathbb{I}$ is to shift all eigenvalues of \mathbf{L}_b by ϵ (i.e. $\lambda_i \rightarrow \lambda_i + \epsilon$) but to leave all the eigenvectors $\mathbf{u}^{(i)}$ unchanged. For $\epsilon > 0$ \mathbf{L}_b is non singular and one readily obtains Eq. (9) for its inverse. \square

Proposition 2. *Under the transformation $\mathbf{L}_b \rightarrow \mathbf{L}_b + \epsilon \mathbb{I}$ with $\epsilon > 0$, the system defined by Eq. (3) is asymptotically stable and has no marginally stable mode.*

Proof. For $\epsilon > 0$, $\mathbf{L}_b + \epsilon \mathbb{I}$ is positive definite. Under this condition, Ref. [20] showed that all eigenvalues of \mathbf{A} have a negative real part. \square

Under the transformation of Proposition 2, Eq. (8) is sufficient to define the observability Gramian with no additional constraint. In this approach we take the limit $\epsilon \rightarrow 0$ at the end of the calculation of a performance measure to recover the physically relevant quantities.

The quadratic performance measure \mathcal{P} can be expressed as the \mathcal{L}_2 norm $\mathcal{P} = \int_0^\infty \mathbf{y}^\top(t) \mathbf{y}(t) dt \equiv \|\mathbf{y}\|_{\mathcal{L}_2}$ of the system's output $\mathbf{y}(t) = \sqrt{\mathbf{Q}^M} [\delta \boldsymbol{\theta}(t), \bar{\boldsymbol{\omega}}(t)]^\top$. Eqs. (3) and (5) together with $\mathbf{y}(t)$ define an input/output system which we denote by

$G = (\mathbf{A}, \mathbf{B}, \sqrt{\mathbf{Q}^M})$. The squared \mathcal{H}_2 norm $\|G\|_{\mathcal{H}_2}^2$ measures the sum of the system's responses to Dirac- δ impulses at every node, $\|G\|_{\mathcal{H}_2}^2 = \sum_i \mathcal{P}^{(i)}$, where $\mathcal{P}^{(i)}$ is the \mathcal{L}_2 norm of the system's output for a Dirac- δ impulse at node i (i.e. $\delta \mathbf{p}^{(i)}(t) = \delta(t) \hat{\mathbf{e}}_i$ for $i = 1, \dots, N$). This quantity is easy to evaluate in terms of the observability Gramian and is given by the trace

$$\|G\|_{\mathcal{H}_2}^2 = \text{Tr}[\mathbf{B}^\top \mathbf{X} \mathbf{B}]. \quad (10)$$

In the formalism we just outlined, the difficulty of evaluating performance measures resides in solving the Lyapunov equation for the observability Gramian \mathbf{X} . Despite some specific choices of \mathbf{Q} for which analytical solutions have been found – see in particular Refs. [11]–[13] for \mathbf{Q} corresponding to resistive losses and primary control effort – this task is generally performed numerically. In the case of generic performance measures little is known about the solutions of the Lyapunov equation. The next section fills this gap by explicitly deriving an analytical expression for the observability Gramian in terms of the eigenvectors of $\mathbf{M}^{-1/2} \mathbf{L}_b \mathbf{M}^{-1/2}$. We then show how our results allow to relate performance measures of the type \mathcal{P} of Eq. (6) to the network topology.

IV. CLOSED FORM EXPRESSION FOR THE OBSERVABILITY GRAMIAN

Proposition 3. *Let \mathbf{A} be a non symmetric, diagonalizable matrix with eigenvalues $\mu_i \neq 0$. Let \mathbf{T}_R (\mathbf{T}_L) denote the matrix whose columns (rows) are the right (left) eigenvectors of \mathbf{A} . The observability Gramian \mathbf{X} , solution of the Lyapunov Eq. (8) is given by*

$$X_{ij} = \sum_{l,q} \frac{-1}{\mu_l + \mu_q} (\mathbf{T}_L)_{li} (\mathbf{T}_L)_{qj} (\mathbf{T}_R^\top \mathbf{Q}^M \mathbf{T}_R)_{lq}. \quad (11)$$

Proof. By definition, \mathbf{T}_L and \mathbf{T}_R fulfill the bi-orthogonality condition $\mathbf{T}_L \mathbf{T}_R = \mathbb{I}$, thus $\mathbf{T}_L \mathbf{A} \mathbf{T}_R = \boldsymbol{\mu}$ with $\boldsymbol{\mu} = \text{diag}(\{\mu_i\})$. Using this transformation in Eq. (8) one has

$$\bar{\boldsymbol{\mu}} \bar{\mathbf{X}} + \bar{\mathbf{X}} \boldsymbol{\mu} = -\mathbf{T}_R^\top \mathbf{Q}^M \mathbf{T}_R, \quad \bar{\mathbf{X}} = \mathbf{T}_R^\top \mathbf{X} \mathbf{T}_R, \quad (12)$$

which yields

$$\bar{\mathbf{X}}_{lq} = \frac{-1}{\mu_l + \mu_q} (\mathbf{T}_R^\top \mathbf{Q}^M \mathbf{T}_R)_{lq}. \quad (13)$$

Finally, using $\mathbf{X} = \mathbf{T}_L^\top \bar{\mathbf{X}} \mathbf{T}_L$ one obtains Eq. (11). \square

Since Proposition 3 holds for $\mu_i \neq 0 \forall i$, it is satisfied by the matrix \mathbf{A} defined in Eq. (3) under the transformation of Proposition 2. We note that Eqs. (11) and (13) are ill defined if one takes the limit $\epsilon \rightarrow 0$. In what follows we assume $\epsilon \neq 0$ and take the limit $\epsilon \rightarrow 0$ only after computing performance measures. Next we relate the explicit expression of the observability Gramian, Eq. (11), to the eigenvectors of $\mathbf{M}^{-1/2} \mathbf{L}_b \mathbf{M}^{-1/2}$.

Assumption 1. *All synchronous machines have uniform damping over inertia ratios $d_i/m_i = \gamma \forall i$.*

Proposition 4. *Consider the power system model defined in Eq. (3) under Assumption 1. The left and right transformation*

matrices \mathbf{T}_L and \mathbf{T}_R diagonalizing \mathbf{A} are related to the eigenvectors of $\mathbf{M}^{-1/2}\mathbf{L}_b\mathbf{M}^{-1/2}$ through the linear transformations given in Eqs. (19) and (20).

Proof. We assume $d_i/m_i = \gamma \forall i$, while still allowing inertias to be different from one synchronous machine to the other. Under this assumption one has that $\mathbf{M}^{-1}\mathbf{D} = \gamma\mathbb{I}$. Thus $\mathbf{M}^{-1}\mathbf{D}$ and $\mathbf{M}^{-1/2}\mathbf{L}_b\mathbf{M}^{-1/2}$ commute and have a common basis of eigenvectors. Since $\mathbf{M}^{-1/2}\mathbf{L}_b\mathbf{M}^{-1/2}$ is symmetric, it has a real spectrum with eigenvalues denoted by λ_i^M , and it is diagonalized by an orthogonal matrix \mathbf{T}_M

$$\mathbf{T}_M^\top (\mathbf{M}^{-1/2}\mathbf{L}_b\mathbf{M}^{-1/2}) \mathbf{T}_M = \mathbf{\Lambda}_M := \text{diag}(\{\lambda_i^M\}). \quad (14)$$

The transformation

$$\begin{bmatrix} \mathbf{T}_M^\top & 0 \\ 0 & \mathbf{T}_M^\top \end{bmatrix} \mathbf{A} \begin{bmatrix} \mathbf{T}_M & 0 \\ 0 & \mathbf{T}_M \end{bmatrix} = \begin{bmatrix} 0 & \mathbb{I} \\ -\mathbf{\Lambda}_M & -\gamma\mathbb{I} \end{bmatrix} \quad (15)$$

leads after index reordering to a matrix with a block diagonal structure composed of 2×2 blocks of the form

$$\begin{bmatrix} 0 & 1 \\ -\lambda_i^M & -\gamma \end{bmatrix}. \quad (16)$$

Diagonalizing the 2×2 blocks, Eq. (16), one obtains the eigenvalues of \mathbf{A} ,

$$\mu_i^\pm = \frac{1}{2}(-\gamma \pm \Gamma_i), \quad \Gamma_i = \sqrt{\gamma^2 - 4\lambda_i^M}, \quad (17)$$

for $i = 1, \dots, N$. From the right and left eigenvectors of Eq. (16) one readily obtains the full transformation which diagonalizes \mathbf{A} ,

$$\mathbf{T}_L \mathbf{A} \mathbf{T}_R = \begin{bmatrix} \text{diag}(\{\mu_i^+\}) & 0 \\ 0 & \text{diag}(\{\mu_i^-\}) \end{bmatrix}, \quad (18)$$

with $\mathbf{T}_L \mathbf{T}_R = \mathbb{I}$,

$$\mathbf{T}_R = \begin{bmatrix} \mathbf{T}_M & 0 \\ 0 & \mathbf{T}_M \end{bmatrix} \begin{bmatrix} \text{diag}(\{1/\sqrt{\Gamma_j}\}) & \text{diag}(\{i/\sqrt{\Gamma_j}\}) \\ \text{diag}(\{\mu_j^+/\sqrt{\Gamma_j}\}) & \text{diag}(\{i\mu_j^-/\sqrt{\Gamma_j}\}) \end{bmatrix}, \quad (19)$$

and

$$\mathbf{T}_L = \begin{bmatrix} \text{diag}(\{-\mu_j^-/\sqrt{\Gamma_j}\}) & \text{diag}(\{1/\sqrt{\Gamma_j}\}) \\ \text{diag}(\{-i\mu_j^+/\sqrt{\Gamma_j}\}) & \text{diag}(\{i/\sqrt{\Gamma_j}\}) \end{bmatrix} \begin{bmatrix} \mathbf{T}_M^\top & 0 \\ 0 & \mathbf{T}_M^\top \end{bmatrix}. \quad (20)$$

□

Eqs. (19) and (20) relate the eigenvectors of \mathbf{A} to those of $\mathbf{M}^{-1/2}\mathbf{L}_b\mathbf{M}^{-1/2}$. This allows to express the observability Gramian of Eq. (11) in terms of the eigenvectors of $\mathbf{M}^{-1/2}\mathbf{L}_b\mathbf{M}^{-1/2}$.

The linearity of the Lyapunov Eq. (8) with respect to both \mathbf{X} and \mathbf{Q}^M implies that for performance measures involving both frequency and voltage phase degrees of freedom [i.e. both $\mathbf{Q}^{(1,1)} \neq 0$ and $\mathbf{Q}^{(2,2)} \neq 0$ in Eq. (4)], the observability Gramian is given by a linear combination of two observability Gramians, each obtained solving a separate Lyapunov equation. Thus, without loss of generality, we address separately two classes of performance measures: those involving frequency degrees of freedom only and those involving phase degrees of freedom only. We note that from Eqs. (5), (6) and (10) it is clear that only the $\mathbf{X}^{(2,2)}$ block of the observability Gramian is relevant to evaluate \mathcal{L}_2 and squared \mathcal{H}_2 norms.

Proposition 5 (Observability Gramian for frequency based performance measures). Consider the power system model defined in Eq. (3) and satisfying Proposition 2. Under Assumption 1, the $\mathbf{X}^{(2,2)}$ block of the observability Gramian associated with the quadratic performance measure defined in Eq. (4) with $\mathbf{Q}^{(1,1)} = 0$, and $\mathbf{Q}^{(2,2)} \neq 0$ is given by

$$X_{ij}^{(2,2)} = \sum_{l,q=1}^N (T_M)_{il} (T_M^\top)_{qj} (T_M^\top \mathbf{M}^{-1/2} \mathbf{Q}^{(2,2)} \mathbf{M}^{-1/2} T_M)_{lq} \times \left[\frac{\gamma(\lambda_l^M + \lambda_q^M)}{2\gamma^2(\lambda_l^M + \lambda_q^M) + (\lambda_q^M - \lambda_l^M)^2} \right], \quad (21)$$

where λ_l^M and \mathbf{T}_M are the eigenvalues and the orthogonal matrix diagonalizing $\mathbf{M}^{-1/2}\mathbf{L}_b\mathbf{M}^{-1/2}$ respectively.

Proof. Inserting Eqs. (19) and (20) into Eq. (11), under the assumption that $\mathbf{Q}^{(1,1)} = 0$ and taking the indices $i, j \in \{N+1, \dots, 2N\}$ to access $\mathbf{X}^{(2,2)}$ yields

$$X_{ij}^{(2,2)} = \sum_{\substack{l,q=1 \\ n,p=1}}^N \frac{(T_M^\top)_{li} (T_M^\top)_{qj} (T_M)_{nl} (T_M)_{pq} Q_{np}^{(2,2)}}{\sqrt{m_n m_p} \Gamma_l \Gamma_q} \times \left[\frac{\mu_q^+ \mu_l^-}{\mu_l^- + \mu_q^+} + \frac{\mu_q^- \mu_l^+}{\mu_l^+ + \mu_q^-} - \frac{\mu_q^+ \mu_l^+}{\mu_l^+ + \mu_q^+} - \frac{\mu_q^- \mu_l^-}{\mu_l^- + \mu_q^-} \right],$$

which simplifies to Eq. (21) using Eq. (17). □

Proposition 6 (Observability Gramian for phase based performance measures). Consider the power system model defined in Eq. (3) and satisfying Proposition 2. Under Assumption 1, the $\mathbf{X}^{(2,2)}$ block of the observability Gramian associated with the quadratic performance measure defined in Eq. (4) with $\mathbf{Q}^{(1,1)} \neq 0$, and $\mathbf{Q}^{(2,2)} = 0$ is given by

$$X_{ij}^{(2,2)} = \sum_{l,q=1}^N (T_M)_{il} (T_M^\top)_{qj} (T_M^\top \mathbf{M}^{-1/2} \mathbf{Q}^{(1,1)} \mathbf{M}^{-1/2} T_M)_{lq} \times \left[\frac{2\gamma}{2\gamma^2(\lambda_l^M + \lambda_q^M) + (\lambda_q^M - \lambda_l^M)^2} \right], \quad (22)$$

where λ_l^M and \mathbf{T}_M are the eigenvalues and the orthogonal matrix diagonalizing $\mathbf{M}^{-1/2}\mathbf{L}_b\mathbf{M}^{-1/2}$ respectively.

Proof. Inserting Eqs. (19) and (20) into Eq. (11), under the assumption that $\mathbf{Q}^{(2,2)} = 0$ and taking the indices $i, j \in \{N+1, \dots, 2N\}$ to access $\mathbf{X}^{(2,2)}$ yields

$$X_{ij}^{(2,2)} = \sum_{\substack{l,q=1 \\ n,p=1}}^N \frac{(T_M^\top)_{li} (T_M^\top)_{qj} (T_M)_{nl} (T_M)_{pq} Q_{np}^{(1,1)}}{\sqrt{m_n m_p} \Gamma_l \Gamma_q} \times \left[\frac{1}{\mu_l^- + \mu_q^+} + \frac{1}{\mu_l^+ + \mu_q^-} - \frac{1}{\mu_l^+ + \mu_q^+} - \frac{1}{\mu_l^- + \mu_q^-} \right],$$

which simplifies to Eq. (22) using Eq. (17). □

Eqs. (21) and (22) are explicit expressions for the observability Gramian valid for generic performance measures. Similar expressions were recently derived in Ref. [21] working in the Laplace frequency domain. For performance measures involving both frequency and phase degrees of freedom, the

observability Gramian is given by a linear combination of Eqs. (21) and (22). We note that the results of Propositions 4, 5, and 6 obtained for the model defined in Eq. (1) generalize to a different class of 2nd order coupled oscillator models involving relative damping $\sum_j -d_{ij}(\dot{\theta}_i - \dot{\theta}_j)$ as opposed to absolute damping $-d_i\dot{\theta}_i$. Such models have been used to describe vehicle platoon formations with relative position and relative velocity feedback [6], [12], [22]. The corresponding observability Gramians are given in Appendix IX.

V. PERFORMANCE MEASURES

We next illustrate how our general expressions for the observability Gramian, Eqs. (21) and (22), can be applied to a variety of performance measures. To do that we first reproduce the results of Refs. [11], [12] and [13]. As a side product our results clarify the mathematical mechanism by which specific parameter choices lead to performance measures \mathcal{P} or squared \mathcal{H}_2 norms that no longer depend on the network topology, a somehow surprising observation in Refs. [11] and [13].

1) *Primary control effort*: Ref. [13] defines the primary control effort as $\mathcal{P} = \int_0^\infty \sum_i d_i \omega_i^2 dt$. Injecting $\mathbf{Q}^{(1,1)} = 0$, $\mathbf{Q}^{(2,2)} = \mathbf{D}$ into Eq. (21), and recalling that $\mathbf{M}^{-1/2} \mathbf{D} \mathbf{M}^{-1/2} = \gamma \mathbb{I}$, gives

$$X_{ij}^{(2,2)} = \sum_{l,q=1}^N \left[\frac{(T_M)_{il} (T_M^\top)_{qj} (T_M^\top T_M)_{lq} \gamma^2 (\lambda_l^M + \lambda_q^M)}{2\gamma^2 (\lambda_l^M + \lambda_q^M) + (\lambda_q^M - \lambda_l^M)^2} \right]. \quad (23)$$

Using $T_M^\top T_M = T_M T_M^\top = \mathbb{I}$, Eq. (23) simplifies to

$$\mathbf{X}^{(2,2)} = \frac{1}{2} \mathbb{I}, \quad (24)$$

and leads to the squared \mathcal{H}_2 norm $\|G\|_{\mathcal{H}_2}^2 = 1/2 \sum_i m_i^{-1}$, in agreement with Ref. [13].

2) *Transmission losses*: Under the assumption of uniform inertias (i.e. $m_i \equiv m$, and $d_i = m_i \gamma \equiv d \forall i$), Ref. [12] evaluates the transmission losses incurred during a transient by computing the squared \mathcal{H}_2 norm of the system, for the performance measure $\mathbf{Q}^{(1,1)} = \mathbf{L}_g$, $\mathbf{Q}^{(2,2)} = 0$ with

$$\mathbf{L}_g = \sum_{\langle \alpha, \beta \rangle} g_{\alpha\beta} \mathbf{e}_{(\alpha,\beta)} \mathbf{e}_{(\alpha,\beta)}^\top. \quad (25)$$

In Eq. (25), $\langle \alpha, \beta \rangle$ denotes all pairs of nodes connected by a resistive line of conductance $g_{\alpha\beta}$. For uniform inertias, $\mathbf{M}^{-1/2} \mathbf{L}_b \mathbf{M}^{-1/2}$ and \mathbf{L}_b have the same eigenvectors, $T_M \equiv T$, with eigenvalues differing by a division with m , $\lambda_i^M \equiv \lambda_i/m \forall i$. The uniform inertia assumption also simplifies the computation of the squared \mathcal{H}_2 norm to

$$\|G\|_{\mathcal{H}_2}^2 = \text{Tr}[\mathbf{B}^\top \mathbf{X} \mathbf{B}] = m^{-1} \text{Tr}[\mathbf{X}^{(2,2)}]. \quad (26)$$

Computing $\text{Tr}(\mathbf{X}^{(2,2)})$ from Eqs. (22) and (25) yields

$$\begin{aligned} \text{Tr}[\mathbf{X}^{(2,2)}] &= \sum_{\langle \alpha, \beta \rangle} g_{\alpha\beta} \sum_{i,l,q} (T)_{il} (T^\top)_{qi} (\mathbf{T}^\top \mathbf{e}^{(\alpha,\beta)} \mathbf{e}^{(\alpha,\beta)\top} \mathbf{T})_{lq} \\ &\quad \times \left[\frac{2\gamma}{2\gamma^2 (\lambda_l + \lambda_q) + (\lambda_q - \lambda_l)^2/m} \right] \\ &= \frac{1}{2\gamma} \sum_{\langle \alpha, \beta \rangle} g_{\alpha\beta} \sum_{l=1}^N \lambda_l^{-1} [(T)_{\alpha l} - (T)_{\beta l}]^2, \\ &= \frac{1}{2\gamma} \sum_{\langle \alpha, \beta \rangle} g_{\alpha\beta} \sum_{l \geq 2}^N \lambda_l^{-1} (u_\alpha^{(l)} - u_\beta^{(l)})^2, \end{aligned} \quad (27)$$

where we used $\mathbf{T} \mathbf{T}^\top = \mathbb{I}$ and $u_i^{(1)} = 1/\sqrt{N} \forall i$ to drop the $l = 1$ term in the sum before taking the limit $\epsilon \rightarrow 0$. Combining Eqs. (26) and (27) we finally reproduce the result of Ref. [12]

$$\|G\|_{\mathcal{H}_2}^2 = \frac{1}{2d} \sum_{\langle \alpha, \beta \rangle} g_{\alpha\beta} \Omega_{\alpha\beta}, \quad (28)$$

where $\Omega_{\alpha\beta}$ is the effective resistance distance between nodes α and β computed with respect to \mathbf{L}_b . In the limit of homogeneous lines (i.e. $g_{\alpha\beta}/b_{\alpha\beta} \equiv r/x$ for all lines), Eq. (28) further simplifies to $\|G\|_{\mathcal{H}_2}^2 = (1/2d)(r/x)(N-1)$ in agreement with Ref. [11]. Remarkably, $\|G\|_{\mathcal{H}_2}^2$ depends on the total number N of nodes but not on the network topology in that case.

3) *Phase coherence*: The performance measure $\mathcal{P} = \int_0^\infty \delta \boldsymbol{\theta}^\top \delta \boldsymbol{\theta} dt$ quantifies the integrated global voltage phase deviation from the nominal operating point during a transient. We evaluate it under the assumption of uniform inertias (i.e. $T_M \equiv T$ and $\lambda_i^M = \lambda_i/m$) and for transients induced by a power injection pulse. In this case, we have $\mathbf{Q}^{(1,1)} = \mathbb{I}$, $\mathbf{Q}^{(2,2)} = 0$, $\delta \mathbf{p}(t) = \delta(t) \hat{\mathbf{e}}_s$ and $\mathbf{B} = [0, m^{-1/2} \hat{\mathbf{e}}_s]^\top$ for a power injection impulse at node s . The observability Gramian, Eq. (22) becomes

$$X_{ij}^{(2,2)} = \frac{1}{2\gamma} \sum_{l=1}^N \lambda_l^{-1} (T)_{il} (T^\top)_{lj} \Rightarrow \mathbf{X}^{(2,2)} = \frac{1}{2\gamma} \mathbf{L}_b^{-1}, \quad (29)$$

where \mathbf{L}_b^{-1} is defined in Proposition 1. We obtain

$$\mathcal{P}^{(s)} = \frac{1}{2d} \left[\epsilon^{-1} u_s^{(1)2} + \sum_{l \geq 2}^N (\lambda_l + \epsilon)^{-1} u_s^{(l)2} \right]. \quad (30)$$

The superscript in $\mathcal{P}^{(s)}$ specifies that we are computing the response to a perturbation occurring at node s and $u^{(l)}$ is the l^{th} eigenvector of \mathbf{L}_b . The marginally stable mode of \mathbf{A} implies that this quantity diverges as the regularizing parameter $\epsilon \rightarrow 0$. We instead compute the difference $\mathcal{P}^{(s)} - \mathcal{P}^{(t)}$ for which the two divergences cancel

$$\mathcal{P}^{(s)} - \mathcal{P}^{(t)} = \frac{1}{2dN} \left[\sum_i \Omega_{si} - \sum_i \Omega_{ti} \right], \quad (31)$$

where we have used that $u_i^{(1)} = 1/\sqrt{N} \forall i$, and that $\sum_i \Omega_{si} = N \sum_{l \geq 2} \lambda_l^{-1} u_s^{(l)2} + \sum_{l \geq 2} \lambda_l^{-1}$. The quantity $N^{-1} \sum_i \Omega_{si}$ entering Eq. (31) is the average resistance distance separating node s from the rest of the network. Its inverse is known as the closeness centrality [16]. From Eq. (31) one concludes that the

difference $\mathcal{P}^{(s)} - \mathcal{P}^{(t)}$ is positive (negative) if the centrality of node t is greater (smaller) than that of node s . In other terms, power fluctuations occurring at nodes which are more central have a smaller impact on the voltage phase fluctuations during the transient.

The examples discussed above illustrate how for specific parameter choices the expressions for the performance measures simplify because of the orthogonality of the eigenvectors of \mathbf{L}_b . This sometimes leads to results that no longer depend on the topology of the network. For instance, this occurs for i) the transmission losses measure, Eq. (25), when ii) inertias are assumed uniform, for iii) Dirac- δ perturbations averaged over all nodes of the network as captured by the squared \mathcal{H}_2 norm, and iv) for lines having constant susceptance over conductance ratio. If any one of these four assumptions is relaxed, the performance measure depends nontrivially on the topology of the network.

VI. PERFORMANCE MEASURES UNDER LINE CONTINGENCIES: FORMALISM

The formalism outlined above can be applied to more general perturbations than the power injection fluctuations considered so far. We consider nonsingular single line faults that do not split the network into two disconnected parts, and introduce a time dependent network Laplacian

$$\mathbf{L}_b(t) = \mathbf{L}_b - \delta(t)b_{\alpha\beta}\mathbf{e}_{(\alpha,\beta)}\mathbf{e}_{(\alpha,\beta)}^\top, \quad (32)$$

which describes an infinitesimally short fault of the $\alpha - \beta$ line at $t = 0$.

The results presented so far rely on the assumption that all nodes of the network are governed by the swing dynamics of Eq. (1), i.e. all nodes have synchronous machines with inertia. In real power networks however, some so-called *passive* nodes are inertialess. Kron reduction allows to eliminate passive nodes and to formulate the dynamics of the network in terms of a swing equation, similar to Eq. (1), involving only the voltage phases of the synchronous machines, all with a finite inertia, on an effective network. For a review of Kron reduction, we refer the reader to Refs. [23] and [24].

To characterize the transient behavior resulting from a line contingency, we first need to formulate how a line fault in the physical network, Eq. (32), impacts the swing dynamics of the Kron reduced network of synchronous machines. If we denote by $\mathcal{N}_g = \{1, \dots, g\}$ and $\mathcal{N}_c = \{g+1, \dots, N\}$ the node subsets representing synchronous machines and passive nodes respectively, we rewrite the DC power flow equation in the physical network as

$$\begin{bmatrix} \mathbf{P}_g \\ \mathbf{P}_c \end{bmatrix} = \begin{bmatrix} \mathbf{L}_b^{(g,g)} & \mathbf{L}_b^{(g,c)} \\ \mathbf{L}_b^{(c,g)} & \mathbf{L}_b^{(c,c)} \end{bmatrix} \begin{bmatrix} \boldsymbol{\theta}_g^* \\ \boldsymbol{\theta}_c^* \end{bmatrix}, \quad (33)$$

where $\mathbf{L}_b^{(g,g)}$, $\mathbf{L}_b^{(g,c)}$, $\mathbf{L}_b^{(c,g)}$ and $\mathbf{L}_b^{(c,c)}$ are blocks of the Laplacian \mathbf{L}_b . Applying Kron reduction to Eq. (33) to eliminate $\boldsymbol{\theta}_c^*$ yields

$$\underbrace{\mathbf{P}_g - \mathbf{L}_b^{(g,c)}\mathbf{L}_b^{(c,c)^{-1}}\mathbf{P}_c}_{\mathbf{P}_{\text{red}}} = \underbrace{\left[\mathbf{L}_b^{(g,g)} - \mathbf{L}_b^{(g,c)}\mathbf{L}_b^{(c,c)^{-1}}\mathbf{L}_b^{(c,g)}\right]}_{\mathbf{L}_{\text{red}}}\boldsymbol{\theta}_g^*. \quad (34)$$

Starting from the physical injections \mathbf{P}_g , \mathbf{P}_c and the physical network with Laplacian \mathbf{L}_b , Eq. (34) defines an effective vector of power injections \mathbf{P}_{red} and an effective Laplacian \mathbf{L}_{red} on a reduced graph [23]. The swing dynamics on the reduced graph reads

$$\mathbf{M}\ddot{\boldsymbol{\theta}}_g = -\mathbf{D}\dot{\boldsymbol{\theta}}_g + \mathbf{P}_{\text{red}} - \mathbf{L}_{\text{red}}\boldsymbol{\theta}_g, \quad (35)$$

with $\mathbf{M} = \text{diag}(\{m_i\})$ and $\mathbf{D} = \text{diag}(\{d_i\})$ for $i \in \mathcal{N}_g$. Because Kron reduction has eliminated all passive nodes, all remaining nodes have inertia.

When discussing transients resulting from line contingencies, it is natural to question how a line fault in the physical network, Eq. (32), affects the swing dynamics of the Kron reduced network Eq. (35). This analysis requires to distinguish three cases:

1) *The faulted line connects two synchronous machines:*

In this case $\alpha, \beta \in \mathcal{N}_g$ and the fault, Eq. (32), only affects the $\mathbf{L}_b^{(g,g)}$ block of the Laplacian \mathbf{L}_b . In terms of \mathbf{L}_{red} and \mathbf{P}_{red} the fault is described by

$$\mathbf{P}_{\text{red}} \rightarrow \mathbf{P}_{\text{red}}, \quad \mathbf{L}_{\text{red}} \rightarrow \mathbf{L}_{\text{red}} - \delta(t)b_{\alpha\beta}\mathbf{e}_{(\alpha,\beta)}\mathbf{e}_{(\alpha,\beta)}^\top, \quad (36)$$

where $\mathbf{e}_{(\alpha,\beta)} \in \mathbb{R}^{|\mathcal{N}_g|}$. The swing equation (35), relative to the nominal operating point $\boldsymbol{\theta}_g(t) = \boldsymbol{\theta}_g^* + \delta\boldsymbol{\theta}_g(t)$, becomes

$$\mathbf{M}\delta\ddot{\boldsymbol{\theta}}_g = -\mathbf{D}\delta\dot{\boldsymbol{\theta}}_g - \mathbf{L}_{\text{red}}\delta\boldsymbol{\theta}_g + \delta(t)b_{\alpha\beta}\mathbf{e}_{(\alpha,\beta)}\mathbf{e}_{(\alpha,\beta)}^\top(\boldsymbol{\theta}_g^* + \delta\boldsymbol{\theta}_g). \quad (37)$$

With the initial condition $(\delta\boldsymbol{\theta}_g(0), \boldsymbol{\omega}_g(0)) = (0, 0)$, the solution to Eq. (37) is

$$\begin{bmatrix} \delta\bar{\boldsymbol{\theta}}_g(t) \\ \bar{\boldsymbol{\omega}}_g(t) \end{bmatrix} = e^{\mathbf{A}t} \underbrace{\begin{bmatrix} 0 \\ \mathbf{M}^{-1/2}b_{\alpha\beta}\mathbf{e}_{(\alpha,\beta)}\mathbf{e}_{(\alpha,\beta)}^\top\boldsymbol{\theta}_g^* \end{bmatrix}}_{\mathbf{B}}, \quad (38)$$

where $\delta\bar{\boldsymbol{\theta}}_g = \mathbf{M}^{1/2}\delta\boldsymbol{\theta}_g$, $\bar{\boldsymbol{\omega}}_g = \mathbf{M}^{1/2}\boldsymbol{\omega}_g$, and \mathbf{A} is the matrix defined in Eq. (3) with \mathbf{L}_b appropriately replaced by \mathbf{L}_{red} .

2) *The faulted line connects two passive nodes:* In this case $\alpha, \beta \in \mathcal{N}_c$ and the fault only affects the $\mathbf{L}_b^{(c,c)}$ block of the Laplacian \mathbf{L}_b while the blocks $\mathbf{L}_b^{(g,g)}$, $\mathbf{L}_b^{(g,c)}$ and $\mathbf{L}_b^{(c,g)}$ remain unchanged. This impacts both \mathbf{L}_{red} and \mathbf{P}_{red} which become

$$\begin{aligned} \mathbf{P}_{\text{red}} &\rightarrow \mathbf{P}_{\text{red}} - \delta(t)b_{\alpha\beta} \frac{\mathbf{L}_b^{(g,c)}[\mathbf{L}_b^{(c,c)}]^{-1}\mathbf{e}_{(\alpha,\beta)}\mathbf{e}_{(\alpha,\beta)}^\top[\mathbf{L}_b^{(c,c)}]^{-1}\mathbf{P}_c}{1 - b_{\alpha\beta}\mathbf{e}_{(\alpha,\beta)}^\top[\mathbf{L}_b^{(c,c)}]^{-1}\mathbf{e}_{(\alpha,\beta)}}, \\ \mathbf{L}_{\text{red}} &\rightarrow \mathbf{L}_{\text{red}} - \delta(t)b_{\alpha\beta} \frac{\mathbf{L}_b^{(g,c)}[\mathbf{L}_b^{(c,c)}]^{-1}\mathbf{e}_{(\alpha,\beta)}\mathbf{e}_{(\alpha,\beta)}^\top[\mathbf{L}_b^{(c,c)}]^{-1}\mathbf{L}_b^{(c,g)}}{1 - b_{\alpha\beta}\mathbf{e}_{(\alpha,\beta)}^\top[\mathbf{L}_b^{(c,c)}]^{-1}\mathbf{e}_{(\alpha,\beta)}}, \end{aligned} \quad (39)$$

where $\mathbf{e}_{(\alpha,\beta)} \in \mathbb{R}^{|\mathcal{N}_c|}$, and where we used the Sherman-Morrison formula [25]

$$\begin{aligned} [\mathbf{L}_b^{(c,c)} - b_{\alpha\beta}\mathbf{e}_{(\alpha,\beta)}\mathbf{e}_{(\alpha,\beta)}^\top]^{-1} &= [\mathbf{L}_b^{(c,c)}]^{-1} \\ &+ b_{\alpha\beta} \frac{[\mathbf{L}_b^{(c,c)}]^{-1}\mathbf{e}_{(\alpha,\beta)}\mathbf{e}_{(\alpha,\beta)}^\top[\mathbf{L}_b^{(c,c)}]^{-1}}{1 - b_{\alpha\beta}\mathbf{e}_{(\alpha,\beta)}^\top[\mathbf{L}_b^{(c,c)}]^{-1}\mathbf{e}_{(\alpha,\beta)}}, \end{aligned} \quad (40)$$

to express the inverse of the rank-1 perturbation of $\mathbf{L}_b^{(c,c)}$. Injecting Eqs. (39) in Eq. (35), and solving the swing equation with initial conditions $(\delta\theta_g(0), \omega_g(0)) = (0, 0)$ yields

$$\begin{bmatrix} \overline{\delta\theta}_g(t) \\ \overline{\omega}_g(t) \end{bmatrix} = e^{\mathbf{A}t} \underbrace{\begin{bmatrix} 0 \\ \frac{-b_{\alpha\beta} \mathbf{M}^{-1/2} \mathbf{L}_b^{(g,c)} [\mathbf{L}_b^{(c,c)}]^{-1} \mathbf{e}_{(\alpha,\beta)} \mathbf{e}_{(\alpha,\beta)}^\top \boldsymbol{\theta}_c^*}{1 - b_{\alpha\beta} \mathbf{e}_{(\alpha,\beta)}^\top [\mathbf{L}_b^{(c,c)}]^{-1} \mathbf{e}_{(\alpha,\beta)}} \end{bmatrix}}_{\mathbf{B}}, \quad (41)$$

where $\overline{\delta\theta}_g = \mathbf{M}^{1/2} \delta\theta_g$, $\overline{\omega}_g = \mathbf{M}^{1/2} \omega_g$, and \mathbf{A} is the matrix defined in Eq. (3) with \mathbf{L}_b replaced by \mathbf{L}_{red} .

3) *The faulted line connects a synchronous machine and a passive node:* In this case $\alpha \in \mathcal{N}_g$ and $\beta \in \mathcal{N}_c$, and the four blocks of \mathbf{L}_b change according to

$$\begin{aligned} \mathbf{L}_b^{(g,g)} &\rightarrow \mathbf{L}_b^{(g,g)} - b_{\alpha\beta} \hat{\mathbf{e}}_\alpha \hat{\mathbf{e}}_\alpha^\top, \\ \mathbf{L}_b^{(c,c)} &\rightarrow \mathbf{L}_b^{(c,c)} - b_{\alpha\beta} \hat{\mathbf{e}}_\beta \hat{\mathbf{e}}_\beta^\top, \\ \mathbf{L}_b^{(c,g)} &\rightarrow \mathbf{L}_b^{(c,g)} + b_{\alpha\beta} \hat{\mathbf{e}}_\beta \hat{\mathbf{e}}_\alpha^\top, \\ \mathbf{L}_b^{(g,c)} &\rightarrow \mathbf{L}_b^{(g,c)} + b_{\alpha\beta} \hat{\mathbf{e}}_\alpha \hat{\mathbf{e}}_\beta^\top, \end{aligned} \quad (42)$$

where $\hat{\mathbf{e}}_\alpha \in \mathbb{R}^{|\mathcal{N}_g|}$ and $\hat{\mathbf{e}}_\beta \in \mathbb{R}^{|\mathcal{N}_c|}$. \mathbf{P}_{red} and \mathbf{L}_{red} become

$$\begin{aligned} \mathbf{P}_{\text{red}} &\rightarrow \delta(t) b_{\alpha\beta} \frac{[\hat{\mathbf{e}}_\alpha + \mathbf{L}_b^{(g,c)} [\mathbf{L}_b^{(c,c)}]^{-1} \hat{\mathbf{e}}_\beta] \hat{\mathbf{e}}_\beta^\top [\mathbf{L}_b^{(c,c)}]^{-1} \mathbf{P}_c}{1 - b_{\alpha\beta} [\mathbf{L}_b^{(c,c)}]_{\beta\beta}^{-1}}, \\ \mathbf{L}_{\text{red}} &\rightarrow \delta(t) b_{\alpha\beta} \frac{[\hat{\mathbf{e}}_\alpha + \mathbf{L}_b^{(g,c)} [\mathbf{L}_b^{(c,c)}]^{-1} \hat{\mathbf{e}}_\beta] [\hat{\mathbf{e}}_\alpha^\top + \hat{\mathbf{e}}_\beta^\top [\mathbf{L}_b^{(c,c)}]^{-1} \mathbf{L}_b^{(c,g)}]}{1 - b_{\alpha\beta} [\mathbf{L}_b^{(c,c)}]_{\beta\beta}^{-1}}, \end{aligned} \quad (43)$$

where, again, we used the Sherman-Morrison formula [25] to compute the inverse of $\mathbf{L}_b^{(c,c)} - b_{\alpha\beta} \hat{\mathbf{e}}_\beta \hat{\mathbf{e}}_\beta^\top$. Finally, injecting Eqs. (43) in Eq. (35), and solving the swing equation with initial conditions $(\delta\theta_g(0), \omega_g(0)) = (0, 0)$ yields

$$\begin{bmatrix} \overline{\delta\theta}_g(t) \\ \overline{\omega}_g(t) \end{bmatrix} = e^{\mathbf{A}t} \underbrace{\begin{bmatrix} 0 \\ \frac{b_{\alpha\beta} \mathbf{M}^{-1/2} (\hat{\mathbf{e}}_\alpha + \mathbf{L}_b^{(g,c)} [\mathbf{L}_b^{(c,c)}]^{-1} \hat{\mathbf{e}}_\beta) (\theta_{g,\alpha}^* - \theta_{c,\beta}^*)}{1 - b_{\alpha\beta} [\mathbf{L}_b^{(c,c)}]_{\beta\beta}^{-1}} \end{bmatrix}}_{\mathbf{B}}, \quad (44)$$

where $\overline{\delta\theta}_g = \mathbf{M}^{1/2} \delta\theta_g$, $\overline{\omega}_g = \mathbf{M}^{1/2} \omega_g$, and \mathbf{A} is the matrix defined in Eq. (3) with \mathbf{L}_b replaced by \mathbf{L}_{red} .

Having solved the swing equation for the three types of line faults we are now ready to present our main results.

Proposition 7 (Phase coherence under line contingency). Consider the Kron reduced power system model of Eq. (35) satisfying Proposition 2, Assumption 1, and $m_i = m \forall i \in \mathcal{N}_g$. The phase coherence measure $\mathcal{P} = \int_0^\infty \delta\theta_g^\top \delta\theta_g dt$ evaluated for a line contingency modeled by Eq. (32) is given by

$$\mathcal{P} = \frac{[b_{\alpha\beta} (\theta_{g,\alpha}^* - \theta_{g,\beta}^*)]^2}{2d} \Omega_{\alpha\beta}, \quad (45)$$

if the faulted line connects two synchronous machines, by

$$\mathcal{P} = \frac{[b_{\alpha\beta} (\theta_{c,\alpha}^* - \theta_{c,\beta}^*)]^2}{2d} \frac{\Omega_{\alpha\beta} - \mathbf{e}_{(\alpha,\beta)}^\top [\mathbf{L}_b^{(c,c)}]^{-1} \mathbf{e}_{(\alpha,\beta)}}{[1 - b_{\alpha\beta} \mathbf{e}_{(\alpha,\beta)}^\top [\mathbf{L}_b^{(c,c)}]^{-1} \mathbf{e}_{(\alpha,\beta)}]^2}, \quad (46)$$

if the faulted line connects two passive nodes, and by

$$\mathcal{P} = \frac{[b_{\alpha\beta} (\theta_{g,\alpha}^* - \theta_{c,\beta}^*)]^2}{2d} \frac{\Omega_{\alpha\beta} - [\mathbf{L}_b^{(c,c)}]_{\beta\beta}^{-1}}{[1 - b_{\alpha\beta} [\mathbf{L}_b^{(c,c)}]_{\beta\beta}^{-1}]^2}, \quad (47)$$

if the faulted line connects a synchronous machine α and a passive node β . In Eqs. (45)–(47), $\Omega_{\alpha\beta}$ is the resistance distance computed with respect to the physical network \mathbf{L}_b , prior to Kron reduction.

Proof. The observability Gramian associated to the phase coherence measure is given in Eq. (29) and is the inverse of the reduced Laplacian \mathbf{L}_{red} . To compute \mathcal{P} for the three types of line contingencies, we use \mathbf{B} defined in Eqs. (38), (41) and (44) respectively and the matrix block inversion property [26]

$$\begin{aligned} (\mathbf{L}_b^{-1})^{(c,c)} &= [\mathbf{L}_b^{(c,c)}]^{-1} + [\mathbf{L}_b^{(c,c)}]^{-1} \mathbf{L}_b^{(c,g)} \mathbf{L}_{\text{red}}^{-1} \mathbf{L}_b^{(g,c)} [\mathbf{L}_b^{(c,c)}]^{-1} \\ [\mathbf{L}_b^{-1}]^{(g,c)} &= -\mathbf{L}_{\text{red}}^{-1} \mathbf{L}_b^{(g,c)} [\mathbf{L}_b^{(c,c)}]^{-1}, \\ [\mathbf{L}_b^{-1}]^{(c,g)} &= [\mathbf{L}_b^{-1}]^{(g,c)\top}, \quad [\mathbf{L}_b^{-1}]^{(g,g)} = \mathbf{L}_{\text{red}}^{-1}. \end{aligned} \quad (48)$$

Eq. (48) holds for \mathbf{L}_{red} regularized according to Proposition 2. Eqs. (45)–(47) are obtained after some algebra, and taking the limit $\epsilon \rightarrow 0$ at the end of the calculation. \square

The results of Proposition 7 show that for the three types of line contingencies, the voltage phase deviation from the nominal operating point is proportional to the square of the power flowing on the line prior to the fault, times a topological factor. The latter is equal to the resistance distance when the faulted line connects two synchronous machines, Eq. (45). For the other two types of line faults, Eqs. (46) and (47), the resistance distance factor of Eq. (45) is complemented by terms which account for the topology of the network of passive nodes, with no straightforward interpretation, except for the term $\mathbf{e}_{(\alpha,\beta)}^\top [\mathbf{L}_b^{(c,c)}]^{-1} \mathbf{e}_{(\alpha,\beta)}$ in Eq. (46), which is equal to the resistance distance between α and β in the network of passive nodes augmented by a ground node (see Th. 3.9 of Ref. [23]).

Proposition 8 (Primary control effort under line contingency). Consider the Kron reduced power system model of Eq. (35) satisfying Proposition 2 and Assumption 1. The primary control effort $\mathcal{P} = \int_0^\infty \sum_i d_i \omega_i^2 dt$ required during the transient caused by a line contingency modeled by Eq. (32) is given by

$$\mathcal{P} = \frac{[b_{\alpha\beta} (\theta_{g,\alpha}^* - \theta_{g,\beta}^*)]^2}{2} (m_\alpha^{-1} + m_\beta^{-1}), \quad (49)$$

if the faulted line connects two synchronous machines, by

$$\begin{aligned} \mathcal{P} &= \frac{[b_{\alpha\beta} (\theta_{c,\alpha}^* - \theta_{c,\beta}^*)]^2}{2} \\ &\times \frac{\mathbf{e}_{(\alpha,\beta)}^\top [\mathbf{L}_b^{(c,c)}]^{-1} \mathbf{L}_b^{(c,g)} \mathbf{M}^{-1} \mathbf{L}_b^{(g,c)} [\mathbf{L}_b^{(c,c)}]^{-1} \mathbf{e}_{(\alpha,\beta)}}{[1 - b_{\alpha\beta} \mathbf{e}_{(\alpha,\beta)}^\top [\mathbf{L}_b^{(c,c)}]^{-1} \mathbf{e}_{(\alpha,\beta)}]^2}, \end{aligned} \quad (50)$$

if the faulted line connects two passive nodes, and by

$$\begin{aligned} \mathcal{P} &= \frac{[b_{\alpha\beta} (\theta_{g,\alpha}^* - \theta_{c,\beta}^*)]^2}{2} \\ &\times \frac{[\hat{\mathbf{e}}_\alpha^\top + \hat{\mathbf{e}}_\beta^\top [\mathbf{L}_b^{(c,c)}]^{-1} \mathbf{L}_b^{(c,g)}] \mathbf{M}^{-1} [\hat{\mathbf{e}}_\alpha + \mathbf{L}_b^{(g,c)} [\mathbf{L}_b^{(c,c)}]^{-1} \hat{\mathbf{e}}_\beta]}{[1 - b_{\alpha\beta} [\mathbf{L}_b^{(c,c)}]_{\beta\beta}^{-1}]^2}, \end{aligned} \quad (51)$$

if the faulted line connects a synchronous machine α and a passive node β .

Proof. The observability Gramian associated to the primary control effort is given in Eq. (24). To compute $\mathcal{P} = \mathbf{B}^\top \mathbf{X} \mathbf{B}$ for the above three types of lines contingencies, we use \mathbf{B} defined in Eqs. (38), (41) and (44) respectively. \square

Eq. (49) shows that the effort of primary control which results from the outage of the $\alpha - \beta$ line is proportional to the square of the power flowing on the line prior to the fault times the prefactor $(m_\alpha^{-1} + m_\beta^{-1})$. The latter indicates that the primary control effort is large if the rotational inertias of the synchronous machines at both ends of the faulted line are small. For the other types of line contingencies, Eqs. (50) and (51) predict a more involved dependence of \mathcal{P} with the inertias of the synchronous machines. Quite interestingly, for both Eqs. (50) and (51), only the inertias of the synchronous machines directly connected to the passive nodes matter. This is easily seen writing $\mathbf{M}^{-1} = \sum_i m_i^{-1} \hat{\mathbf{e}}_i \hat{\mathbf{e}}_i^\top$ for $\hat{\mathbf{e}}_i \in \mathbb{R}^{|\mathcal{N}_g|}$ and noticing that $\mathbf{L}_b^{(c,g)} \hat{\mathbf{e}}_i = 0$ if the i^{th} synchronous machine is not connected to any of the passive nodes.

VII. PERFORMANCE MEASURES UNDER LINE CONTINGENCIES: NUMERICAL ANALYSIS

To illustrate our results we perform numerical investigations taking as physical network the IEEE-118 testcase [28]. Assuming that PQ buses are passive, we simulate the swing dynamics for the reduced model, Eq. (35), where all PQ buses have been eliminated by Kron reduction. To model temporary line disconnections, we consider time-dependent network Laplacians,

$$\mathbf{L}_b(t) = \mathbf{L}_b + \Theta(t)\Theta(\tau - t)b_{\alpha\beta}\mathbf{e}_{(\alpha,\beta)}\mathbf{e}_{(\alpha,\beta)}^\top, \quad (52)$$

where $\Theta(t)$ is the Heavyside step function, τ is the clearing time, and $\alpha - \beta$ is the faulted line. We perform numerical simulations for all possible line contingencies in the network, each time evaluating numerically the performance measures $\int_0^\infty \sum_i \delta\theta_i^2(t) dt$ and $\int_0^\infty \sum_i d_i\omega_i^2(t) dt$. We compare the numerical results to our theoretical predictions. Since the latter hold for Dirac- δ perturbations [see Eq. (32)], our theoretical results are expected to be accurate for small clearing times as $\delta(t) = \lim_{\tau \rightarrow 0} \Theta(t)\Theta(\tau - t)/\tau$.

Fig. 1, shows the behavior of the phase coherence measure rescaled by the square of the power flowing on the line prior to the fault for all lines connecting two synchronous machines in the physical network. As predicted for homogeneous inertias and sufficiently short clearing times, Eq. (45), this quantity is linear in the resistance distance. The validity of the observability Gramian prediction for Dirac- δ perturbations extends to longer clearing times for larger inertia of the synchronous machines (red crosses). This is so because voltage phase oscillations are more easily absorbed locally by larger inertia. These results show that for longer clearing times, and more generally for perturbations that are extended in time, alternative approaches to the observability Gramian are needed to accurately evaluate performance measures [29].

Fig. 2, shows the behavior of the primary control effort rescaled by the square of the power flowing on the line prior to the fault for all lines connecting two synchronous machines in the physical network. For heterogeneous inertias

and sufficiently short clearing times we expect, according to Eq. (49), that this quantity scales linearly with $(m_\alpha^{-1} + m_\beta^{-1})$. This prediction is confirmed for sufficiently large inertias. For lower values of inertia, the linear tendency holds for short clearing times, but breaks down for longer faults. The red crosses in Figs. 1 and 2 correspond to somehow exaggerated values of inertia. They are here to illustrate that our theoretical predictions have larger domain of applicability in the presence of larger inertias.

Finally, Fig. 3 shows the phase coherence and the primary control effort measures for all possible line contingencies (170 lines in total, of which 46 connect two synchronous machines, 35 connect two passive nodes and 89 connect a passive node to a synchronous machine) and $\tau = 20$ ms. The transmission lines are sorted according to the square of the power flowing on the line in normal operation. Numerical results confirm that our theoretical predictions are accurate indicators of transient vulnerability under line contingency and that the transient excursion is given by the square of the power flowing on the transmission line prior to the fault times a topological factor for the phase coherence measure [Eqs. (45)–(47)] or an inertia dependent factor for the primary control effort [Eqs. (49)–(51)].

Remarkably, our results show that the transient performance under line fault is not a monotonic function of the power load of the faulted line, the square of which is indicated by the black line in Fig. 3. Both the network topology and the distribution of inertia in the grid strongly impact the transients. We observe that the most critical lines are not always the most highly loaded ones. For the phase coherence measure (left panel in Fig. 3), the line carrying the 6th largest power leads to the largest integrated transient excursions even though it carries 30% less power than the line carrying the most power. We saw (but do not show here) this non monotonic behavior also when lines are sorted according to their relative load (the load relative to their capacity). A similar non monotonicity is observed for the primary control effort (right panel in Fig. 3). The fault of the line carrying the 3rd largest power causes the largest primary control effort, and the line carrying 44% of the largest transmitted power (line ranked 14th with respect to absolute load) is the 4th most critical one.

VIII. CONCLUSION

The standard formalism used until now to evaluate performance measures of electric power grids was restricted to nodal perturbations [11]–[13] and we extended it to line perturbations. We showed numerically that, despite its restriction to Dirac- δ perturbation (instantaneous in time), the formalism correctly evaluates performance measures even in the physically relevant case of perturbations with finite, but not too long duration. One would naively guess that the most critical lines are those that are the most heavily loaded, either relatively to their thermal limit or in absolute value. Quite surprisingly, we found that faults on lines transmitting less than half of the heaviest line load in the network require more primary effort control or perturb the network's coherence more than lines with higher loads. This is so, because performance

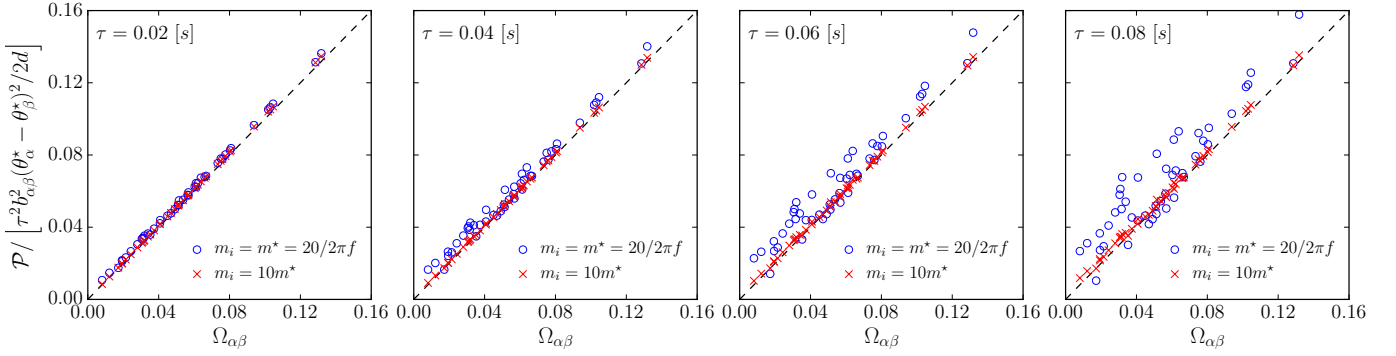


Fig. 1. Voltage phase variance (from the nominal operating point) incurred during a transient resulting from a line contingency as a function of the resistance distance separating the nodes of the faulted line. Each data point corresponds to the fault of a line connecting two generators in the physical network. Simulation parameters: IEEE-118 testcase with uniform inertia at all nodes, $f = 50$ Hz, $d_i/m_i = 0.5$ [s⁻¹], and $m_i = m^* = 2H/2\pi f$, $H = 10$ [s] (typical values from [27], blue circles) and $m_i = 10m^*$ (red crosses). From left to right: fault clearing times τ corresponding to 1, 2, 3, and 4 AC cycles. The straight line gives our theoretical prediction Eq. (45).

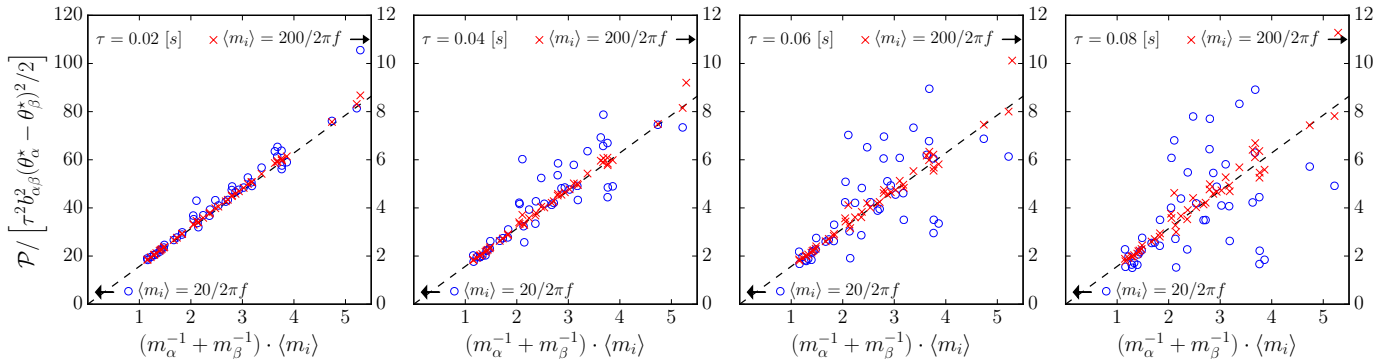


Fig. 2. Primary control effort required during a transient resulting from a line contingency as a function of the sum of the inverse inertias of the synchronous machines at both ends of the faulted line. Each data point corresponds to the fault of a line connecting two generators in the physical network. Simulation parameters: IEEE-118 testcase with inertias uniformly distributed in the interval $[0.2\langle m \rangle, 1.8\langle m \rangle]$ with $\langle m \rangle = 2H/2\pi f$, $H = 10$ [s] (typical values from [27], blue circles) and $\langle m \rangle = 200/2\pi f$ (red crosses), $f = 50$ Hz, and $d_i/m_i = 0.5$ [s⁻¹]. From left to right: fault clearing times τ corresponding to 1, 2, 3, and 4 AC cycles. The straight line gives our theoretical prediction Eq. (49).

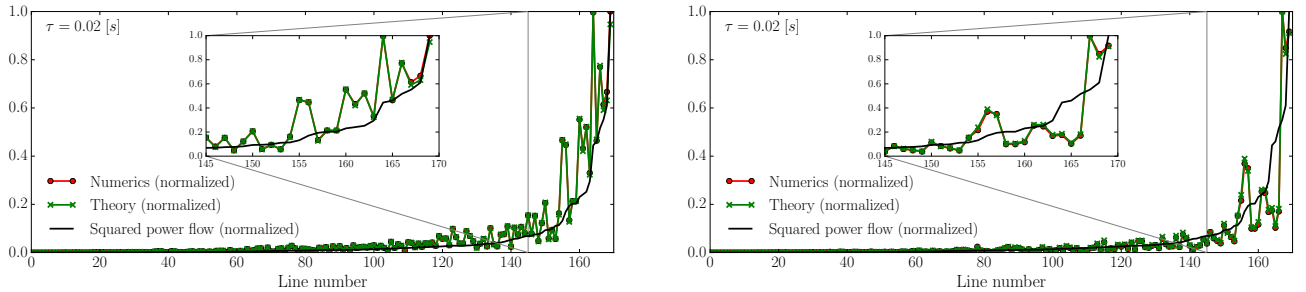


Fig. 3. Plot of the normalized performance measure (red), theoretical prediction (green), and square of the power flowing on the line prior to the fault (black) for line contingencies with clearing times $\tau = 0.02$ [s]. Transmission lines are ordered according to the power flowing on the line prior to the fault. Left panel: phase coherence measure, uniform inertias $m_i = m^* = 2H/2\pi f$, $H = 10$ [s], $f = 50$ Hz, and $d_i/m_i = 0.5$ [s⁻¹]. Right panel: primary control effort, inertias uniformly distributed in the interval $[0.2\langle m \rangle, 1.8\langle m \rangle]$ with $\langle m \rangle = 2H/2\pi f$, $H = 10$ [s], $f = 50$ Hz, and $d_i/m_i = 0.5$ [s⁻¹].

measures, Eqs. (45)–(47) and Eqs. (49)–(51), are given by the square of the original load on the faulted line times a term depending on the topology of the network. The performance measures we calculated could therefore be used in $N - 1$ contingency analysis to quickly identify the most critical lines, based on topological characteristics of the network together with the load they carry.

Future works should investigate nodal $N - 1$ faults, where a bus with all its connected lines is removed from the network.

At present this seems to be hard to calculate as such a fault is difficult to map from the physical to the Kron reduced network.

ACKNOWLEDGMENT

We thank B. Bamieh for useful discussions. This work was supported by the Swiss National Science Foundation under an AP Energy Grant.

IX. APPENDIX

Proposition 9 (Oscillators with relative damping). *Consider the 2^{nd} order, coupled oscillator model with relative damping*

$$\mathbf{M}\ddot{\mathbf{x}} = -\mathbf{L}_d\dot{\mathbf{x}} + \mathbf{P} - \mathbf{L}_b\mathbf{x}, \quad (53)$$

where $\mathbf{M} = \text{diag}(\{m_i\})$ and both \mathbf{L}_b and \mathbf{L}_d are Laplacian matrices associated to the network of coupling and damping interactions. If the matrices $\mathbf{M}^{-1/2}\mathbf{L}_b\mathbf{M}^{-1/2}$ and $\mathbf{M}^{-1/2}\mathbf{L}_d\mathbf{M}^{-1/2}$ commute, the observability Gramians of Propositions 5 and 6 generalize to

$$X_{ij}^{(2,2)} = \sum_{l,q=1}^N (T_M)_{il} (T_M^\top)_{qj} \left(T_M^\top \mathbf{M}^{-1/2} \mathbf{Q}^{(2,2)} \mathbf{M}^{-1/2} T_M \right)_{lq} \times \left[\frac{(\eta_q^M \lambda_l^M + \eta_l^M \lambda_q^M)}{(\eta_q^M + \eta_l^M)(\eta_q^M \lambda_l^M + \eta_l^M \lambda_q^M) + (\lambda_q^M - \lambda_l^M)^2} \right] \quad (54)$$

and

$$X_{ij}^{(2,2)} = \sum_{l,q=1}^N (T_M)_{il} (T_M^\top)_{qj} \left(T_M^\top \mathbf{M}^{-1/2} \mathbf{Q}^{(1,1)} \mathbf{M}^{-1/2} T_M \right)_{lq} \times \left[\frac{(\eta_q^M + \eta_l^M)}{(\eta_q^M + \eta_l^M)(\eta_q^M \lambda_l^M + \eta_l^M \lambda_q^M) + (\lambda_q^M - \lambda_l^M)^2} \right] \quad (55)$$

where λ_l^M and T_M are the eigenvalues and the orthogonal matrix diagonalizing $\mathbf{M}^{-1/2}\mathbf{L}_b\mathbf{M}^{-1/2}$, and η_l^M are the eigenvalues of $\mathbf{M}^{-1/2}\mathbf{L}_d\mathbf{M}^{-1/2}$.

Proof. Since $\mathbf{M}^{-1/2}\mathbf{L}_b\mathbf{M}^{-1/2}$ and $\mathbf{M}^{-1/2}\mathbf{L}_d\mathbf{M}^{-1/2}$ commute they have common eigenvectors T_M . The results of Proposition 4 generalize simply replacing γ by η_l^M in Eqs. (17), (19) and (20). The $X^{(2,2)}$ block of the observability Gramian is calculated analogously as in Propositions 5 and 6 to obtain Eqs. (54) and (55). \square

REFERENCES

- [1] Y. Kuramoto, *Lecture Notes in Physics*, vol. 39, pp. 420–422, 1975.
- [2] A. Pikovsky, M. Roseblum, and K. J. Synchronization: A Universal Concept in Nonlinear Sciences. Cambridge University Press, 2001.
- [3] J. Machowski, J. W. Bialek, and J. R. Bumby, *Power system dynamics: stability and control*. John Wiley, 2008.
- [4] “Power systems of the future: The case for energy storage, distributed generation, and microgrids,” IEEE Smart Grid, Tech. Rep. Nov. 2012.
- [5] S. Backhaus and M. Chertkov, “Getting a grip on the electrical grid,” *Phys. Today*, vol. 66, no. 5, pp. 42–48, 2013.
- [6] B. Bamieh, M. R. Jovanovic, P. Mitra, and S. Patterson, “Coherence in large-scale networks: Dimension-dependent limitations of local feedback,” *IEEE Transactions on Automatic Control*, vol. 57, no. 9, pp. 2235–2249, 2012.
- [7] T. Summers, I. Shames, J. Lygeros, and F. Dörfler, “Topology design for optimal network coherence,” in *European Control Conference*. IEEE, 2015, pp. 575–580.
- [8] M. Siami and N. Motew, “Systemic measures for performance and robustness of large-scale interconnected dynamical networks,” in *53rd Annual Conference on Decision and Control*. IEEE, 2014, pp. 5119–5124.
- [9] M. Fardad, F. Lin, and M. R. Jovanovic, “Design of optimal sparse interconnection graphs for synchronization of oscillator networks,” *IEEE Transactions on Automatic Control*, vol. 59, no. 9, pp. 2457–2462, 2014.
- [10] K. Zhou, J. Doyle, and K. Glover, “Robust and optimal control,” 1996.
- [11] E. Tegling, B. Bamieh, and D. F. Gayme, “The price of synchrony: Evaluating the resistive losses in synchronizing power networks,” *IEEE Transactions on Control of Network Systems*, vol. 2, no. 3, pp. 254–266, 2015.

- [12] T. W. Grunberg and D. F. Gayme, “Performance measures for linear oscillator networks over arbitrary graphs,” *IEEE Transactions on Control of Network Systems*, vol. PP, no. 99, pp. 1–1, 2016.
- [13] B. K. Poolla, S. Bolognani, and F. Dörfler, “Optimal placement of virtual inertia in power grids,” *IEEE Transactions on Automatic Control*, vol. PP, no. 99, pp. 1–1, 2017.
- [14] D. J. Klein and M. Randić, “Resistance distance,” *Journal of Mathematical Chemistry*, vol. 12, no. 1, pp. 81–95, 1993.
- [15] K. Stephenson and M. Zelen, “Rethinking centrality: Methods and examples,” *Social Networks*, vol. 11, no. 1, pp. 1 – 37, 1989.
- [16] E. Bozzo and M. Franceschet, “Resistance distance, closeness, and betweenness,” *Social Networks*, vol. 35, no. 3, pp. 460 – 469, 2013.
- [17] D. J. Klein, “Graph geometry, graph metrics and Wiener,” *Commun. Math. Comput. Chem.*, no. 35, pp. 7–27, 1997.
- [18] W. Xiao and I. Gutman, “Resistance distance and laplacian spectrum,” *Theoretical Chemistry Accounts*, vol. 110, no. 4, pp. 284–289, 2003.
- [19] T. Coletta and P. Jacquod, “Resistance distance criterion for optimal slack bus selection,” *arXiv preprint arXiv:1707.02845*, 2017.
- [20] —, “Linear stability and the braess paradox in coupled-oscillator networks and electric power grids,” *Phys. Rev. E*, vol. 93, p. 032222, Mar 2016.
- [21] F. Paganini and E. Mallada, “Global performance metrics for synchronization of heterogeneously rated power systems: The role of machine models and inertia,” *arXiv preprint arXiv:1710.07195*, 2017.
- [22] F. Lin, M. Fardad, and M. R. Jovanovic, “Optimal control of vehicular formations with nearest neighbor interactions,” *IEEE Transactions on Automatic Control*, vol. 57, no. 9, pp. 2203–2218, 2012.
- [23] F. Dörfler and F. Bullo, “Kron reduction of graphs with applications to electrical networks,” *IEEE Transactions on Circuits and Systems I*, vol. 60, no. 1, pp. 150–163, 2013.
- [24] —, “Spectral analysis of synchronization in a lossless structure-preserving power network model,” in *First IEEE International Conference on Smart Grid Communications*, 2010, pp. 179–184.
- [25] J. Sherman and W. J. Morrison, “Adjustment of an inverse matrix corresponding to a change in one element of a given matrix,” *Ann. Math. Statist.*, vol. 21, no. 1, pp. 124–127, 1950.
- [26] R. A. Horn and C. R. Johnson, *Matrix Analysis*, 2nd ed. New York, NY, USA: Cambridge University Press, 2012.
- [27] P. Kundur, N. J. Balu, and M. G. Lauby, *Power system stability and control*. McGraw-hill New York, 1994, vol. 7.
- [28] U. of Washington, “Power systems testcase archive,” 1993. [Online]. Available: <https://www2.ee.washington.edu/research/pstca>
- [29] M. Tyloo, T. Coletta, and P. Jacquod, “Robustness of synchrony in complex networks and generalized Kirchhoff indices,” *arXiv preprint arXiv:1710.07536*, 2017.

Tommaso Coletta Received the M.Sc. degree in physics and the Ph.D. degree in theoretical physics from the Ecole Polytechnique Fédérale de Lausanne (EPFL), Lausanne, Switzerland in 2009 and 2013 respectively. He has been a Postdoctoral researcher at the Chair of Condensed Matter Theory at the Institute of Theoretical Physics of EPFL. Since 2014 he is a Postdoctoral researcher at the engineering department of the University of Applied Sciences of Western Switzerland, Sion, Switzerland working on complex networks and power systems.

Philippe Jacquod Philippe Jacquod received the Diplom degree in theoretical physics from the ETHZ, Zürich, Switzerland, in 1992, and the PhD degree in natural sciences from the University of Neuchâtel, Neuchâtel, Switzerland, in 1997. He is a professor with the engineering department, University of Applied Sciences of Western Switzerland, Sion, Switzerland. From 2003 to 2005 he was an assistant professor with the theoretical physics department, University of Geneva, Geneva, Switzerland and from 2005 to 2013 he was associate, then full professor with the physics department, University of Arizona, Tucson, USA. Currently, his main research topics is in power systems and how they evolve as the energy transition unfolds. He is co-organizing an international conference series on related topics. He has published about 100 papers in international journals, books and conference proceedings.